

## Excess mixing volume, microstrain, and stability of pyrope-grossular garnets

WEI DU<sup>1,2</sup>, SIMON MARTIN CLARK<sup>3,4</sup>, AND DAVID WALKER<sup>1</sup>

<sup>1</sup>Lamont-Doherty Earth Observatory and Department of Earth and Environmental Sciences,  
Columbia University in the City of New York, Palisades, New York 10964, USA

<sup>2</sup>Present address: Geodynamic Research Center, Ehime University, Matsuyama 790-8577, Japan  
Earth-Life Science Institute, Tokyo Institute of Technology, Tokyo 152-8550, Japan

<sup>3</sup>Department of Earth and Planetary Sciences, Macquarie University, North Ryde, NSW 2109,  
Australia

<sup>4</sup>The Bragg Institute, Australian Nuclear Science and Technology Organization, Locked Bag  
2001, Kirrawee DC, NSW 2232, Australia

### ABSTRACT

Synchrotron X-ray diffraction (XRD) was used to measure the unit cell parameters of synthetic pyrope ( $\text{Mg}_3\text{Al}_2\text{Si}_3\text{O}_{12}$ ), grossular ( $\text{Ca}_3\text{Al}_2\text{Si}_3\text{O}_{12}$ ) and four intermediate garnet solid solutions. Garnets synthesized dry in multi-anvil (MA) apparatus at 6 GPa show irregular asymmetric positive quenchable excess volumes, with binary Margules parameters  $W_{V_{\text{grossular}}} = 2.04 \pm 0.14 \text{ cm}^3/\text{mol}$ , and  $W_{V_{\text{pyrope}}} = 4.47 \pm 0.15 \text{ cm}^3/\text{mol}$ . The two-parameter Margules equation is only an approximate description of the excess volumes in the pyrope-grossular garnets from this study and from the literature. Our values for intermediate garnets are roughly a factor of  $\sim 3$  larger than previous literature reports of excess volumes of garnets grown at piston-cylinder (PC) pressures (2-4 GPa) with hydrothermal assistance. The discrepancy between our large dry excess

volumes and the smaller hydrothermally assisted syntheses previously reported in the literature may be due in part to the hydrothermal assistance. When we do damp syntheses, we too get small excess volume. Although dampness produces smaller excess volumes, the mechanism by which this is achieved remains to be discovered. Does dampness relieve microstrains to relax excess volumes? Analysis of synchrotron X-ray diffraction profiles by using Williamson-Hall plots to test for microstrain shows that peak width does change with dampness and with garnet composition. Microstrain in the garnet structure, rather than grain size variation, is the principal reason for the observed XRD peak broadening. Damp garnets at  $\text{Py}_{60}\text{Gr}_{40}$  have less microstrain and lower excess volume than dry  $\text{Py}_{60}\text{Gr}_{40}$ , in accord with the working hypothesis that dampness is responsible for diminished excess volume through strain relief. However garnets with compositions  $\text{Py}_{80}\text{Gr}_{20}$  and  $\text{Py}_{20}\text{Gr}_{80}$ , close to the negligibly strained end members pyrope ( $\text{Py}_{100}$ ) and grossular ( $\text{Gr}_{100}$ ), have large microstrains but relatively small excess volume. This is in contrast to  $\text{Py}_{40}\text{Gr}_{60}$ , which has the largest excess volume but almost no microstrain. [The end members have no excess volume, by definition, and little microstrain.] This uncorrelated behavior demonstrates that microstrain in general is not directly related to the excess volumes, whatever else dampness may do to a specific composition, for instance introduce a small amount of clinopyroxene into the mode that partitions Ca preferentially away from garnet. Thus the mechanism responsible for the difference between our large excess volumes and the smaller ones in the literature may not be as complete or as simple as dampness relieves microstrain and relaxes excess volume. Our dry intermediate garnets have already been relieved of their microstrain by some other mechanism than dampness and still have large excess volume. The state of Ca-Mg ordering may also change, and we show that this may have a small effect on the excess volume through experiments using variable synthesis time and temperature. A potential

test for whether our large, complex excess volumes, of whatever origin, are real (or not) is whether the rise of the solvus with pressure is better described by our large excess volumes or those smaller ones in the literature. We observe garnet phase exsolution at 8 GPa and show it to be reversible, at a temperature consistent with theoretical calculation using the large mixing volume presented in the current study.

Keywords: Pyrope-grossular garnet solid solution, excess volume, microstrain, garnet exsolution

## INTRODUCTION

Walker et al. (2005) showed that excess volumes ( $V_{ex}$  = difference between measured molar volume and that calculated from the proportional combination of the end-members) of the halite-sylvite solution were strongly temperature and pressure dependent. A binary Margules solution model only approximately describes the volume mixing behavior between solid chloride end-members, and yet the binary Margules approximation provides an accurate prediction of the rise of the solvus with increasing pressure for the join NaCl-KCl. Evaluation of another more complex high-pressure geological solution series, in this case garnet, provides a motivation for this study. Does the Margules form give a good description of a less ionic crystalline solution? [Preview answer: not particularly, like the chlorides.] Does it still provide an adequate basis for predicting the rise or fall of the solvus with pressure? [Preview answer: yes, like the chlorides.]

Pyrope-grossular garnets have a cubic structure as do the chlorides, which make their characterization by X-ray diffraction simpler than for lower symmetry phases. The  $X$  dodecahedral site is occupied by divalent cations Mg and Ca and the biggest polyhedra (e.g. Mg, Ca dodecahedra) in the garnet cell contribute about one third to the cell volume. Unlike pyrope-

almandine substitution of Mg for Fe, which shows near-ideal mixing properties because of the small difference in ionic radii of  $\text{Mg}^{2+}$  and  $\text{Fe}^{2+}$  (0.89 vs. 0.92 Å in 8 coordination) (Shannon 1976), the large size mismatch between divalent  $\text{Mg}^{2+}$  (0.89Å) and  $\text{Ca}^{2+}$  (1.12Å) make pyrope-grossular solid solutions candidates for studies of non-ideal mixing properties (e.g. Newton et al. 1977; Geiger et al. 1987; Wood 1988; Ganguly et al. 1993; Bosenick et al. 1995, 1996, and 1997; Geiger and Feenstra 1997; Dachs and Geiger 2006; Freeman et al. 2006). In addition to the reported large excess volumes along the pyrope-grossular binary at ambient conditions (Fig.1), we observed that the excess mixing volume changes with pressure and temperature (Du et al. 2015). However, details of the mixing of pyrope-grossular garnet are still not clear enough to explain the observed positive mixing excess volume and especially the discrepancies among the various studies.

Newton and Wood (1980), following Iiyama's (1974) "excluded volume" principle, suggested that the larger  $\text{Ca}^{2+}$  cation substituted into a pyrope-rich garnet structure deforms its surrounding structure and creates a "forbidden region" for another  $\text{Ca}^{2+}$  to enter its immediate neighborhood. The garnet structure as a whole does not undergo much expansion, potentially causing negative excess volumes in the pyrope-rich region of the solution. However, later experimental studies found no regions of negative excess volumes along the pyrope-grossular binary, and concluded that the greatest deviations from ideality were located in grossular-rich compositions (e.g. Ganguly et al. 1993; Bosenick and Geiger 1997). Geiger and Feenstra (1997) used a crystal-chemical model with rigid  $\text{SiO}_4$ -tetrahedral rotation to explain the asymmetric excess volumes pattern of the garnet solid solution: the calculated tetrahedral rotation angle along this join displays an analogous asymmetric trend to that of the calculated excess volume but without any negative excess volume. Structure modeling result suggested instead that a

*symmetric* excess volume pattern in pyrope-grossular garnet with a maximum  $\Delta V$  of mixing of  $0.56 \text{ cm}^3/\text{mol}$  for composition  $\text{Py}_{50}\text{Gr}_{50}$  should be found (Ungaretti et al. 1995).

Agreement in the literature on the compositional dependence of the excess volume on the pyrope-grossular join is poor and the reason for the poorly-reproducible, non-linear behavior is not clear. All the previous experimental studies discussed above are based on garnet synthesized at high pressures (3-4 GPa) with some degree of hydrothermal assistance, at less than the dry pressure used this study (6 GPa). Thus the difference in pressure and dampness may be partially responsible for the magnitude and compositional dependence of the differences in excess volumes found by various investigators. It is also possible that partial ordering of cations (Mg and Ca in the dodecahedral site) achieved during synthesis can influence excess volume and can be preserved in the garnet structure during slow decompression after rapid temperature quenching (Hazen and Navrotsky 1996). In fact, some short-range ordering of Mg and Ca in pyrope-grossular solid solutions was confirmed by MAS NMR spectroscopy (Bosenick et al. 1995, 1999; Kelsey et al. 2008), and supported by theoretical calculations (Bosenick et al. 2001; Vinograd et al. 2004; Freeman et al. 2006). However, no short range ordering of Mg and Ca cations was detected in garnets with composition close to the two end members: pyrope and grossular, contradicting Newton and Wood's "forbidden regions" rule which comprises a special type of non-random order.

In addition to excess mixing volume, other properties of the pyrope-grossular garnet solutions, for example the excess mixing enthalpy (Newton et al. 1977), the elastic structural strain (Dapiaggi et al. 2005), and nonlinear compositional dependence of thermo-compression (Du et al. 2015) may also be related to the microstructure changes caused by substitution of Mg and Ca. In this paper, we present molar volumes of pyrope, grossular, and four garnet solid

solutions synthesized dry at 6 GPa with a multi-anvil (MA) device and the XRD profile analysis results. There is a complex correlation between microstrain inside the garnet structure and the nonideal mixing properties along the pyrope-grossular binary. A compositionally dependent degree of short-range Ca-Mg ordering that develops during annealing after MA crystallization may also be partly responsible for the asymmetrical shape of the excess volume in the pyrope-grossular join. We compare our dry systematic results to selected damp experimental tests, and to various annealing strategies for various times for various pyrope-grossular compositions to explore the stability of our garnets with respect to microstructural strain and exsolution behavior.

## EXPERIMENTAL PROCEDURE

### Synthesis of garnet crystals

The set of garnets studied here were synthesized anhydrously from homogeneous glass starting materials in a Walker-type multi anvil device (MA) at Lamont-Doherty Earth Observatory (LDEO). Details of the synthesis procedure and crystals' composition were given by Du et al. (2015) for the same garnets used in the present study. Glasses with six different composition were finely ground, tightly packed into the cylindrical cavity on one side of an S-type (Pt10Rh) thermocouple that bisected the length of a 3 mm inner diameter LaCrO<sub>3</sub> furnace tube within a 8 mm truncated edge length octahedral pressure medium. The cavity on the other side of the thermocouple was filled with an MgO spacer. After this loading, the assembly of anvils was inserted between the driving wedges of the Walker-type multi-anvil pressure-temperature device at LDEO and pressurized to 6 GPa by application of 300 tons force. In order to avoid the crystallization of clinopyroxene, garnets were synthesized at 6 GPa and 1400 °C with only a few seconds residence in the 700-1100 °C temperature interval during heating. Clinopyroxene was observed to crystallize at or below 1100 °C during *in situ* XRD observations

of the crystallization process in a multi-anvil pressure-temperature device at Station 16.4 of the Daresbury, UK Synchrotron Radiation Source (using graphite heaters instead of  $\text{LaCrO}_3$ ). At Daresbury, XRD spectra were observed during real time crystallization with a compound 3-element energy dispersive detection system recording at 3 separate angles from the transmitted beam through the Daresbury horizontal MA. The Daresbury 16.4 facility was described by Clark (1996) and calibrated by Walker et al. (2000, 2002) and Johnson et al. (2001). Refresh rates on the energy dispersive detector system were approximately every 10 seconds. When garnet crystallization is observed *in situ* in the MA environment at 5-6 GPa and temperature  $\sim 1200$  °C, the conversion of glass to garnet takes place in less than 1 minute. The garnets so produced are phase-clean of clinopyroxene *if the heating cycle has avoided lingering in the 700-1100 °C interval*. Garnets synthesized in MA at LDEO were heated for about 30 minutes, and the unit cell volume of garnets grown this way in MA were reproducible. The relative sharpness of the XRD peaks implies that no large component of the garnets' grain size is nanocrystalline, which is confirmed by SEM observation showing that garnet grain size varies from 2 to 10  $\mu\text{m}$ . Compositions of these garnets were checked by microprobe at LDEO and averages of 10 were shown to be the same as the averages for starting glasses and to be homogeneous within the precision of the counting statistics (Du et al. 2015).

Garnets with composition  $\text{Py}_{60}\text{Gr}_{40}$  were synthesized with two different methods: (1) from dried glass with MA device (6 GPa and 1400 °C); and (2) by hydrothermally assisted synthesis methods similar to those used by many other researchers who used piston cylinder devices (Newton et al. 1977, Ganguly et al. 1993, Bosenick et al. 1995). Glass with composition  $\text{Py}_{60}\text{Gr}_{40}$  was sealed with distilled  $\text{H}_2\text{O}$  as a flux in Pt capsules and held at 3 GPa and 1000°C for 5 hours in a piston cylinder device. The product was finely grounded in an agate mortar and used

as crystal seed to mix with dry glass (crystal seed being about 8 wt%). The mixture of glass and crystal seeds was then sealed in Pt capsules (or not, see Table 3) and pressured to 4 GPa and then heated at 1300°C in the multi-anvil device for 2.5-3 hours, giving phase-clean garnet (TT734 and TT736) of smaller cell volume than for the dry synthesis. Seeded glass held at 6 GPa, 1400 °C for only 1 hour (BB941) produced phase-unclean garnet of still smaller cell volume.

To further understand the discrepancies between the piston cylinder (PC) results of the previous studies and our new multi anvil (MA) results, and to study possible partial ordering of Mg and Ca in the dodecahedral site inside the garnet structure, more MA experiments to synthesize garnets at 6 GPa and different temperature and time conditions were done at LDEO. Garnets with composition  $\text{Py}_{80}\text{Gr}_{20}$  (TT890) were synthesized in the MA device at LDEO from the same batch of glass that we used to synthesize pure garnet at 6 GPa and 1400 °C as described above, but heated at 1300 °C and 6 GPa for only 5 minutes and then quenched to room temperature and pressure. The product of this experiment was embedded within KBr powder and put back into the MA device and pressured to 6 GPa and held at 1400 °C for 100 minutes, and then quenched to room temperature and pressure (TT895).

Long-term annealing experiments were conducted at LDEO with MA device to study the stability of pyrope-grossular garnets with respect to exsolution. Starting materials of these annealing experiments are paired garnet crystals synthesized from a mixture of glass particles with two different compositions. Further experiments to effect convergence/divergence of coexisting garnet compositions were conducted in 3 mm diameter rhenium heater tubes instead of  $\text{LaCrO}_3$  to boost the pressure achieved by similar press forces. Garnet grains with paired compositions from the synthesis experiments were put in a position close to S (Pt10Rh) thermocouple junctions that bisected the Re heater tube. KBr powder was put in the heater to

protect the samples from contamination and crushing at high pressure. The reannealed garnets were cleanly recovered from the KBr by aqueous dissolution and their new paired compositions redetermined by XRD through a 4<sup>th</sup> order polynomial relating quenched cell volumes to garnet composition.

### **X-ray diffraction**

The unit cell parameters of garnets synthesized in MA at LDEO were measured at the Advanced Light Source, Lawrence Berkeley National Laboratory (ALS on beamline 12.2.2 at room temperature and pressure, in angular dispersive mode with an MAR345® image plate detector. Garnet chunks or garnet powders were loaded in the ~120  $\mu\text{m}$  diameter hole of a 60  $\mu\text{m}$  thick steel washer typically used as a gasket within a diamond anvil cell (DAC) with the thrust axis parallel to the incident X-ray beam. The present experiments simply mounted the gasket in the X-ray beam without a DAC for support. The diffraction images were obtained using X-ray wavelengths  $\lambda = 0.4133\sim 0.4959$   $\text{\AA}$  (30~25 keV), and the refined distance between sample and the detector (~400 mm) was determined for each run through collection of a standard  $\text{LaB}_6$  diffraction pattern. The X-ray diffraction patterns were collected from  $5^\circ$  to  $30^\circ$   $2\theta$ . The two-dimensional diffraction rings were integrated to one-dimensional diffraction patterns using FIT2D software (Hammersley et al. 1996). XFIT (Cheary and Coelho 1996) and REFCEL (Cockcroft and Barnes 1997) were used to extract the unit cell parameters through peak fitting analysis, which determines the unit cell parameter from least squares analysis of the positions of the peaks.

The unit cell volume of  $\text{Py}_{60}\text{Gr}_{40}$  from two alternate synthesis methods investigating dampness and annealing times and the paired garnet crystals that were used in long-term annealing exsolution experiments and the product of these annealing experiments were checked

with X-ray diffraction measurement using CuK $\alpha$  radiation ( $\lambda=1.540592 \text{ \AA}$ ) on a RIGAKU (46 mV and 40 mA) micro diffractometer with cylindrical image plate detector at the American Museum of Natural History (AMNH).

## RESULT AND DATA ANALYSIS

### Excess volume

The unit cell parameters of end member pyrope and grossular garnets synthesized dry at 6 GPa are consistent with previous studies of pyrope and grossular synthesized at 2-4 GPa with hydrothermal assistance (Table 1). The mixing volumes of pyrope-grossular garnets with intermediate composition were calculated from X-ray diffraction patterns of these solid solution garnets at ambient condition and summarized in column 3 in table 2 and Figure 1. The garnets synthesized dry at 6 GPa show positive excess volumes for the intermediate compositions of the pyrope-grossular garnet series that are substantially greater than for garnets from PC syntheses (Fig. 2). The excess volume pattern of garnet synthesized dry at 6 GPa is asymmetric, with larger values in the grossular-rich garnets. Intermediate garnets (Gr<sub>60</sub>Py<sub>40</sub>) show excess volumes approaching 1.0 cm<sup>3</sup>/mol, which are ~3 times of those previously reported. The molar volumes of end member grossular and pyrope agree well with previous reported values, indicating good inter-laboratory reproducibility for these compositions. The larger excess volumes that we find for intermediate Ca-Mg compositions, that deviate from literature values, are rendered more significant by our agreement with previous studies for the end member values.

A two-parameter Margules equation was fit to the molar volume values of garnet:

$$V(X)_{P,T} = X_{pyrope} \cdot V_0^{pyrope} + X_{grossular} \cdot V_0^{grossular} + X_{pyrope} \cdot X_{grossular} (X_{pyrope} \cdot W_{V_{grossular}} + X_{grossular} \cdot W_{V_{pyrope}}) \quad (1)$$

Where  $V_0^{pyrope}$  and  $V_0^{grossular}$  are the molar volumes of the compositional end-members at room pressure and temperature,  $X_{pyrope}$  and  $X_{grossular}$  are the mole fractions of the respective components of the garnets,  $W_{V_{pyrope}}$  and  $W_{V_{grossular}}$  are the excess volume parameters in the Margules formulation. Hence, excess molar volume can be expressed by the equation:

$$V(X)_{excess P,T} = X_{pyrope} \cdot X_{grossular} (X_{pyrope} \cdot W_{V_{grossular}} + X_{grossular} \cdot W_{V_{pyrope}}) \quad (2)$$

At room temperature and pressure, the Margules equation can be approximately fit to the calculated excess volume data of our MA synthesized garnets (Fig. 1), giving  $W_{V_{pyrope}} = 4.47 \pm 0.15 \text{ cm}^3/\text{mol}$ ,  $W_{V_{grossular}} = 2.04 \pm 0.14 \text{ cm}^3/\text{mol}$ , which is about 3 times that of previous reported results. For example, Ganguly et al. (1993) reported a slightly positive excess volume of mixing on the pyrope-grossular join, which is also skewed toward the grossular end member with Margules parameters of  $W_{V_{pyrope}} = 1.73 \pm 0.30 \text{ cm}^3/\text{mol}$  and  $W_{V_{grossular}} = 0.36 \pm 0.23 \text{ cm}^3/\text{mol}$ . Very similar volumetric behavior was also reported by Bosenick and Geiger (1997). Pyrope-grossular garnets synthesized in the MA and PC devices show the same positive sense of non-ideal asymmetric mixing volume but our new Margules parameter values are 2-3 times larger than the previous garnets synthesized in PC. We note that none of the data from this study or in literature is fit particularly well by the Margules model; and it is difficult to see systematic deviations that would suggest a more appropriate way to model the excess volumes in this series with a single such rationale. The garnets may be more complex than can be accounted for within a single framework. Excess volume may have other determinants than Ca-Mg misfit. These might include dampness, microstrain, presence of other phases, and/or Ca-Mg ordering.

The discrepancy between our dry 6 GPa synthesis results for intermediate pyrope-grossular compositions and previous literature data is striking enough that we wondered whether we could

reproduce literature results for the excess volumes of intermediate compositions if we followed the P-T and dampness recipes from the literature using our starting materials. If we could reproduce literature results of low, positive excess volumes then such features as differences in sample composition between us and the literature, or intrinsic operational characteristics of MA vs. PC synthesis, would be removed from the list of potential causes of the large excess volume discrepancy. With such a finding, dampness would also be implicated as an agent in causing the low excess volumes in the literature.

For these reasons we undertook the experiments on composition  $\text{Py}_{60}\text{Gr}_{40}$  reported in Table 3 and Figure 2, using both dry starting materials and ones that had assistance from hydrothermally grown seeds. We used both our standard 6 GPa and the lower pressures used in the literature of 4 GPa. Figure 2 and Table 3 show that dampness lowers excess volume. All the hydrothermally assisted garnets have smaller cells than their dry counterpart. Thus dampness shows a clear role in reducing excess volume. The amount by which our damp garnets lose excess volume compared to our dry ones resolves a substantial part of the discrepancy between our dry results and those produced by hydrothermally assisted synthesis in the literature. The large scatter in the literature data (shown by the low-excess-volume band) is consistent with dampness being a poorly controlled variable in those studies. It is not well-controlled in our Table 3 data either, hence the scatter of the Table 3 data in Figure 2. We find that the effect of dampness is in the right direction and of the right order to explain the discrepancy between our excess volumes and the literature. It follows that the unexplained excess volume anomaly noted by Ganguly et al. (1993) for  $\text{Gr}_{85}\text{Py}_{15}$  in their experiment JW15 might be explained as a loss of intended dampness. JW15 has an anomalously large excess volume indistinguishable from our dry results.

The mechanism by which dampness reduces excess volume remains to be clarified. One

possible working hypothesis is that any dampness incorporated into garnet by the hydrogrossular substitution removes Si-O-Si bonds and therefore relieves strains associated with the distortion of SiO<sub>4</sub> tetrahedra. Such strains are important in Bosenick et al.'s (2000) treatment of Ca/Mg substitution and ordering. Such strains may also contribute to excess volume until they are relaxed. Therefore we undertook to look at the microstructural strain state of our dry garnets with X-ray profile analysis for comparison to the strain in the hydrothermally assisted garnets of Dapiaggi et al. (2006).

### **XRD peak broadening**

Two ways to define an XRD peak width are: (a) Full width at half maximum (FWHM) ( $\Gamma$ ): the width of the diffraction peak, in radians, at a height halfway between background and the peak maximum [most of the fitting programs give FWHM as XRD peak width]; (b) And Integral Breadth ( $\beta$ ): the total area under the peak divided by the peak intensity, which is the same as the width of a rectangle having the same area and the same height as the peak. The  $\Gamma$  and  $\beta$  for various peak shapes (Lorentzian, Gaussian, Voigt, pseudo-Voigt) can be related with numerical equations (Langford 1978). We found the pseudo-Voigt peak profile best fit our data and used FWHM values from pseudo-Voigt peak profile to determine the XRD peak widths for different garnet compositions along the pyrope-grossular binary.

A close study of the X-ray diffraction patterns of garnet solid solutions synthesized in the MA apparatus at 1400°C and 6 GPa shows that XRD line broadening caused by the mixing between pyrope and grossular end members can be quantified by using synchrotron XRD. Garnet solid solution with intermediate composition shows broader XRD peaks than the two end members, except garnet solid solution with composition Py<sub>40</sub>Gr<sub>60</sub>, which shows similar XRD peak width with end members and do not increase much with  $2\theta$  (Bragg angle) (Fig. 3).

Moreover, garnets with composition near the end members (Py<sub>80</sub>Gr<sub>20</sub> and Py<sub>20</sub>Gr<sub>80</sub>) show much broader peaks than garnets with composition closer to the mid-point of the pyrope-grossular join (Py<sub>60</sub>Gr<sub>40</sub> and Py<sub>40</sub>Gr<sub>60</sub>).

For general XRD patterns, the XRD peaks become broader with  $2\theta$  (Bragg angle). There are a number of reasons for this, for example the angular dispersion of the X-rays, the angular aperture of the detector, and nature of the sample itself. Many of these considerations driving peak broadening are specific to certain laboratory instruments and are not relevant to the ALS synchrotron X-ray source and the ALS XRD image plate detection system. LaB<sub>6</sub> compound has the narrowest peaks of all the materials used in this study and shows little variation from 5° to 30°  $2\theta$  (Fig. 3). Therefore we adopt the measured peak broadening (B) of LaB<sub>6</sub> as the instrumental broadening  $B_{inst} = B_{LaB_6}$ . The sample broadening,  $B_{garnet}$ , can be determined from the measured sample broadening  $B_{obs}$  by equation (3):

$$B_{garnet} = B_{obs} - B_{inst} = B_{obs} - B_{LaB_6} \quad (3)$$

### Williamson-Hall plot

There are many factors that contribute to the observed XRD peak broadening, among which crystallite size and microstrain contributions are strongly  $2\theta$  dependent. The  $2\theta$  dependence of grain size and microstrain is different, which allows us to evaluate the two effects on peak broadening separately by using Williamson-Hall plot (Williamson and Hall 1953):

$$B_{garnet} = B_{size+strain} = B_{obs} - B_{LaB_6} = \frac{K\lambda}{\langle L \rangle \cos \theta} + 4\eta \tan \theta \quad (4)$$

$$B_{garnet} \cos \theta = \frac{K\lambda}{\langle L \rangle \cos \theta} \cos \theta + 4\eta \tan \theta \cos \theta = \frac{K\lambda}{\langle L \rangle} + 4\eta \sin \theta \quad (5)$$

where  $\frac{K\lambda}{\langle L \rangle \cos \theta}$  is the width of the peak due to size effects (Scherrer 1918), K is a constant of value approximately 0.9 (Langford and Wilson 1978), L is the crystal size;  $4\eta \tan \theta$  is the width

of the peak due to microstrain (Stokes and Wilson 1944),  $\eta$  is the microstrain factor,  $\lambda$  is the wavelength of the X-ray, and  $\theta$  is the Bragg angle.

To evaluate the reasons for the broadening peaks in pyrope-grossular garnet, we fit equation (5) to our refined FWHM data for pyrope-grossular garnet solid solutions (Fig. 4). A linear equation was fit to the data, and the slope of this fitting equation is  $4\eta$  in equation (5), which indicates the contribution of microstrain to XRD peak broadening. Theoretically, the intercept on the Y-axis of this fitting equation indicates the contribution of grain size (diffraction domain) to the XRD peak broadening. The estimated grain size of pyrope-grossular solid solution is about 0.5-2 $\mu\text{m}$  from the intercepts in Figure 4, which is too big (>500nm) for reasonable accuracy in estimating grain size (Langford and Wilson 1978). Indeed, the actual grain size is observed to be in the 2-10  $\mu\text{m}$  range. Although we took XRD peak width of  $\text{LaB}_6$  as the standard for instrumentally caused XRD peak widening, which may cause some uncertainty on evaluation of the contribution of grain size to the XRD peak widening, it is very clear that the slope of the fitting equation changes much with composition, showing that microstrain is the principle reason for the peak broadening of these garnet solid solutions. The different slope of the Williamson-Hall plot for different garnet compositions indicates that this microstrain is related to Mg and Ca mixing along the pyrope-grossular binary.

The FWHM for the two end-members, pyrope and grossular, shows little peak broadening even though they were synthesized at the same pressure and temperature conditions as the intermediate compositions (Fig. 3). The XRD peak broadening that we observed in garnet with intermediate compositions would appear to be related to the only remaining variable, Mg-Ca substitution. The XRD peak width shows strong  $2\theta$  dependence, and the  $\eta$  value, which represents the microstrain in garnet structure, shows compositional dependence, indicating that

garnets with composition near to, but not at, the end members carry the most microstrain (Table 2 and Fig. 4).

## DISCUSSION

### Dampness, Ca-Mg, and microstrain

**Table 3** gives the microstrain results found for  $\text{Py}_{60}\text{Gr}_{40}$  synthesized damp and dry. The peak broadening is most pronounced in TT717, the dry synthesis, as compared to the various damp experiments, indicating that it has the most microstrain (Fig. 5). This is consistent with the possibility that dampness lowers excess volume by relieving microstrains (Fig. 6). However this isolated result is difficult to fit into a broader context of variation of excess volume with compositional variation in Ca/Mg that does not include dampness. This broader relation between Ca-Mg and dry microstrain is set out in Figure 6 from the data in Table 2. It is shown that there are substantial variations in dry microstrain with Ca-Mg composition, and that these variations have little to do with excess volume. Excess volumes peak at very modest microstrain and diminish at peak microstrains. The excess volume is zero at the end members (by definition) where the microstrain is also minimal. Evidently microstrain does not have much relation to excess volume in dry garnets even though at one Ca-Mg composition, dampness reduces both microstrain and excess volume. The reduction in microstrain with dampness correlates poorly in detail with the reduction in excess volume. BB941 with the biggest reduction in excess volume reduces its microstrain the least. Thus we are inclined to believe that any connection between microstrain and excess volume is not straightforward, with or without dampness.

Figure 6 also shows the microstrain results of Dapiaggi et al. (2005) in the same series of garnets synthesized by Bosenick et al. (1995) using the hydrothermally assisted seeding technique. There is general agreement about the level of microstrains recovered in the pyrope-

grossular garnets between the two studies, except for the grossular-rich garnets. We show a microstrain peak at  $\text{Py}_{20}\text{Gr}_{80}$ , whereas Dapiaggi et al. (2005) do not. Nevertheless there is no global disconnect between the strain state in our dry garnets and possibly damp ones. Clearly more work is needed to understand the remaining small difference. The two studies differ in details, but is this difference a consequence of dampness or ordering state or noise? We might seek confirmation of our patterns by checking whether or not our microstrain patterns correlate with any other physical properties. Figure 7 shows that there is a good match between the two-peaked microstrain pattern we recover and the two-valley thermal expansion pattern we measured for these same garnets in our companion paper (Du et al. 2015). Likewise Figure 8 suggests that there may also be a significant but somewhat less compelling correlation between our microstrains and the excess enthalpies of Newton et al. (1977). So we doubt that the patterns are just noise. Nevertheless our working hypothesis that dampness relieves microstrain and relaxes excess volume is difficult to sustain, not only from the difficulties that it has with our dry garnet patterns, but also from the conundrum that wet garnets have similar patterns of microstrain with Ca/Mg substitution. The difficulties of discovering exactly what is responsible for our excess volumes suggest that there may be more than one causal agency. We now consider another possible agent.

### **Microstrain and Mg and Ca short-range ordering**

Cation order/disorder can influence unit cell volume and some thermal-compression properties. Although it was reported by previous studies that short range ordering of Mg and Ca contributes to the asymmetric shape of the excess volume in pyrope-grossular garnet (e.g. Bosenick et al. 1999, 2001), the relationship between degree of order and unit cell volume is not well understood because of the lack of information about the details of the disordered/ordered

structure and the potential previously unrecognized effects of dampness. The fact that all unit cell volume data  $V_0$  for pyrope and grossular at ambient condition (which could show Al/Si order/disorder, but not Mg/Ca order/disorder) are in basic agreement no matter whether synthesized in PC or MA (Table 1) makes it reasonable to presume Al and Si order/disorder is not involved in the pyrope-grossular binary. The observation that the two end member garnets carry almost zero microstrain indicates that the microstrain calculated from XRD peak broadening that we observed along the pyrope-grossular join is related to the Mg-Ca substitution. Therefore, if there is short range ordering involved, it is ordering of Mg and Ca cations, and the different degrees of ordering of Mg and Ca cations in the dodecahedral position could be partially responsible for the different peak broadenings and excess volumes observed along the pyrope-grossular binary.

Cation order-disorder may change with synthesis conditions such as temperature, composition, and pressure (Hazen and Navrotsky 1996). For the pyrope-grossular garnet solid solution, the change between disordered and ordered requires Mg and Ca cations to move, and hence is dependent on Ca-Mg diffusion rates. This may be sluggish at high pressure and relatively fast at high temperature in response to changing diffusion rates. In addition, the change in degree of ordering will depend on the time available. Therefore, different synthesis P-T-t conditions could change the degrees of ordering of Mg and Ca that will be achieved in the garnet structure. To test the possible effect of temperature and heating time on XRD peak width (microstrain) and excess volume, we did two more MA experiments at the same pressure (6 GPa) and different times and temperatures (TT889 and TT895) as described above.  $\text{Py}_{80}\text{Gr}_{20}$  garnet crystals synthesized from glass at 1300°C for a short heating time (5 minutes) show a scarcely resolvable, larger unit cell dimension (0.01 Å) and easily resolvable narrower XRD peaks,

compared with those synthesized at 1400 °C for 30 minutes heating by our normal procedure. Reheating this 1300 °C sample (TT889) to 1400 °C for another 100 minutes (TT895) makes their unit cell parameter shrink to the same size as those synthesized at 1400 °C for 30 minutes heating. The 1400 °C samples treated for 100 minutes have the broader XRD peaks, implying more microstrain, characteristic of the higher temperature synthesis (Table 4 and Fig. 9). These are direct experiments showing the correlation between microstrain and annealing temperature: the second round annealing at higher temperature (TT895) caused *increased* microstrain in garnet structure. The fact that longer heating time itself (100 minutes vs 30 minutes) does not cause more microstrain in garnet structure suggests that, in the cases between 1300 and 1400 °C, temperature has more effect on microstrain than annealing time. These three annealed garnets with quite variable microstrains and the same composition have practically indistinguishable volumes, emphasizing the lack of connection between microstrain and molar volume of dry samples.

Among the possible contributions to XRD peak broadening, dislocations, antiphase domain boundaries, and faulting are all *hkl* dependent and are correlated with uniform lattice strain, which then will cause the unit cell to expand/contract in an isotropic way. The peak broadening that we observed in our XRD pattern does not show strong *hkl* dependence, therefore, the most plausible contribution to the microstrain in these garnet structures is non-uniform lattice distortion, which leads to systematic shifts of atoms from their ideal positions (site disorder) and the peak broadening. For a totally disordered structure, Mg and Ca cations have equal opportunities to distribute in all the available dodecahedral sites. However, as discussed by Bosenick et al. (2000) short range ordering of Mg and Ca in pyrope-grossular garnet solid solution derives from the avoidance of a third nearest neighbor Mg-Mg and Ca-Ca pairs

(dodecahedra that are edge-shared with a SiO<sub>4</sub> tetrahedron). Recent *ab initio* calculations further confirmed that the preferential ordering was caused by avoiding Mg-Mg in third nearest neighbor pairs (Freeman et al. 2006). Even though more studies on the local environment of cations are necessary to perform a detailed structural analysis of pyrope-grossular garnets, more and more experimental studies and theoretical calculations agree that garnet with intermediate composition for example Mg:Ca = 50:50 carries some Mg and Ca short range ordering and less distorted SiO<sub>4</sub> tetrahedra, which share edges with these two cations. The atomistic behavior may be related to macroscopic behavior. For example the relatively smaller microstrain that we observed from garnet solid solution Py<sub>40</sub>Gr<sub>60</sub> and the larger microstrain that we observed for garnets with composition close to the end members can then be explained by the different amount of distorted SiO<sub>4</sub> tetrahedra, which indicates that there are more Mg-Mg and Ca-Ca pairs in the third nearest neighbor position for garnets with composition close to the end members.

<sup>29</sup>Si NMR studies on pyrope-grossular garnet by Bosenick et al. (1999) suggested that the degree of Mg and Ca short range ordering decreases with increasing temperature, indicating a more disordered structure at higher temperature and thus more Mg-Mg and Ca-Ca pairs in the third nearest neighbor causing more distorted SiO<sub>4</sub> tetrahedra. This assumption is confirmed by our second round heating experiment (TT895), which shows larger microstrain after reheating at higher temperature (1400°C) (Table 4 and Fig. 9). Therefore, the different peak width that we observed from TT890 and TT895 (Fig. 9) could be due to the different degree of short range ordering of Ca and Mg cations. Here we presume that garnet (Py<sub>80</sub>Gr<sub>20</sub>) synthesized at 1300 °C after 5 minutes heating (TT890) has larger degree of Mg and Ca short range ordering (less Mg-Mg and Ca-Ca pair in the nearest neighbor and less distorted SiO<sub>4</sub> tetrahedra) than those synthesized at 1400 °C for longer annealing time.

## Microstrain and excess volume

The large microstrain within the garnet solid solution that we observe in XRD peak broadening is not directly related to the large positive excess volume on the pyrope-grossular join. The solid solution with composition  $\text{Py}_{40}\text{Gr}_{60}$  shows largest excess volume but almost no microstrain and garnet with composition  $\text{Py}_{80}\text{Gr}_{20}$  shows relatively smaller excess volume but much larger microstrain. At fixed synthesis pressure and temperature, the nature of the anticorrelation between microstrain and excess volume with compositional variation is complex, because we see poor correlation between the single-peaked variation of excess volume with composition in Figure 1 and the two-peaked variation of microstrain with composition in Figure 6. Furthermore, as discussed above, our second round annealing experiment on garnet solid solution  $\text{Py}_{80}\text{Gr}_{20}$  shows that annealing at high temperature caused *more* microstrain in garnet structure, but does not significantly change the lattice parameter. Therefore, the effect of microstrain on excess volume is not important in the dry pyrope-grossular binary.

Can short-range ordering help dampness to resolve the problem of different excess volume of pyrope-grossular garnets synthesized in MA and PC? To make a direct correlation between a larger degree of short-range ordering and relatively larger excess volumes observed in garnets synthesized in the MA, we need to assume that the intermediate Ca-Mg garnets synthesized in the MA are closer to ordering structures than those synthesized in the PC. However, this presumption contradicts the general conclusion that higher temperature will favor a more disordered structure, thus more microstrain and relatively smaller molar volume. In other words, if we only consider the different heating temperatures between our MA garnet (1400 °C) and most PC synthesis garnet (1000-1300°C), and the effect of annealing temperature on order/disorder status of garnet structure, we would expect a more disordered structure of garnet

synthesized with MA and therefore more microstrain and less molar volume. This deduction is opposite to the experimental observation, where MA synthesis garnets with intermediate composition along the pyrope-grossular binary show larger molar volume than those from PC synthesis. In addition, microstrain data of pyrope-grossular garnet synthesized in the PC (Dapiaggi et al. 2005) showed consistency with our MA synthesized garnet that garnet solid solutions with intermediate composition show larger microstrain than the two end members (Fig. 6), indicating that the difference in excess volume cannot be explained by the microstrain with the short range ordering assumption.

We agree with previous studies that the molar volume of pyrope-grossular garnet solid solution is highly non-ideal and positive. However, for those garnets with intermediate composition along the pyrope-grossular binary synthesized with hydrothermal assistance, there is some difference among different groups (Fig. 2). This deviation could be due to the difficulty of synthesizing pure single phase garnet with Ca-rich composition in a PC device as reported by Newton et al. (1977), and later confirmed by Ganguly et al. (1993) that garnet with Ca-rich composition synthesized in PC device was contaminated by some unidentified phase and/or a small amount of clinopyroxene. The contamination of extraneous phases introduces uncertainty in garnet composition, which could also be part of the reason, in addition to poorly controlled dampness, for the different observed excess volumes between garnets synthesized in PC versus MA.

## IMPLICATION

### **The solvus in pyrope-grossular garnet**

Equations in two-parameter Margules form to describe the dependence of critical mixing temperature upon pressure by Thompson (1967) successfully predict the change of the critical

mixing temperature of halite-sylvite solid solution with pressure (Walker et al. 2005). The two-parameter Margules equations should give us a rough estimate of how the solvus of pyrope-grossular garnet will change with pressure. The dependence of the temperature of the consolute point,  $T_C$ , on compositionally weighted functions of the excess enthalpies and excess volumes is described by the following equation (after Walker et al. 2005):

$$\frac{\partial T_C}{\partial P} = T \cdot \frac{W_{Vpyrope} + W_{Vgrossular} - 3(X_{pyrope} \cdot W_{Vgrossular} - X_{grossular} \cdot W_{Vpyrope})}{W_{Hpyrope} + W_{Hgrossular} - 3(X_{pyrope} \cdot W_{Hgrossular} - X_{grossular} \cdot W_{Hpyrope})} \quad (6)$$

Where  $X$  is the molar percentage of the end member component in the garnet solid solution at the consolute point,  $W_V$  is the excess volume parameter for the two components and  $W_H$  is the excess enthalpy parameter. By assuming that the pyrope-grossular mixing properties  $W_H$  are independent of pressure (Ganguly and Kennedy 1974), and the composition of the solid solution at the critical point does not change significantly with pressure, we obtain that  $\frac{\partial T}{\partial P} \propto T \cdot W_V / W_H$ . Although we adopt some simplification in the theoretical calculation, the 3 times larger  $W_V$  we calculate from our new MA garnets implies that the pressure dependence of the temperature of the consolute point should be about 3 times that estimated from the small  $W_V$  of previous studies. For example, by increasing pressure from 0.5 to 4GPa, the critical temperature of the garnet solvus would increase by ~100 °C instead of the ~30 °C that was calculated by Ganguly et al. (1996) who used their relatively smaller excess volume data to estimate how the solvus changes with pressure in a  $X$ - $T$  phase diagram. A value of 6-8 °C/GPa is typical of the expected rise of solvus consolute temperature with pressure based on small, damp excess volumes from the literature. We note that the rise rate of  $T_C$  is also proportional to  $T$  and inversely proportional to the thermal mixing  $W_H$  values (if they vary from investigation to investigation). Indeed the estimated consolution temperatures for the pyrope-grossular solvus range from 400 to as much as

3000 °C (e.g. Ganguly et al. 1996, compared to Haselton and Newton, 1980; or Dachs and Geiger, 1996), all from the small  $W_V$  values of hydrothermally assisted garnets. The large variation in consolute temperature  $T_C$  arises from whether the mixing properties are assumed to be symmetric and what values are used for the thermal mixing properties, there being small variation in the small excess mixing volumes between studies in the literature (See Figure 2). Given this very broad range in estimates of the consolute  $T_C$ , it seemed advisable to test whether any direct evidence of the solvus from coexisting garnet pairs could be found in experiment. The much larger excess volumes in pyrope-grossular garnet presented here imply that the pyrope-grossular solvus can rise in temperature rapidly enough ( $\sim 25$  °C/GPa or more) to possibly become experimentally accessible at higher pressures, perhaps less than 10 GPa. We therefore undertook further annealing experiments to discover whether or not we could directly observe pyrope-grossular thermoconsolution at our multi-anvil-accessible pressure, temperature, and laboratory time scales.

There is a consensus about the approximate consolute compositions among previous investigators which is quite unlike their disparate estimates of consolute  $T_C$ . Haselton and Newton (1980), Ganguly et al. (1996), and Dachs and Geiger (2006) all place the solvus crest between 20 and 40% grossular. This predicted solvus placement is in good accord with the compositional position of natural coexisting garnet pairs reported in the literature by Cressy (1978) and Wang et al. (2000). The solvus is asymmetric, and in the normal sense of having the immiscible compositions closer to the smaller end-member than the larger (as shown by many mineral solutions) cresting at pyrope contents between 60 and 80%. Thus we chose to anneal garnet assemblages with bulk compositions near 65-70% pyrope in the expected consolute composition region. Experiments that produce a single garnet composition from paired garnet

starting materials are at  $T$  above  $T_C$ . [Unless, of course, they are poorly located in composition off the consolute composition.] Experiments that produce paired garnets of wider compositional separation (divergence) than the starting materials are at temperature below  $T_C$ . Experiments that produce paired garnets of smaller compositional separation (convergence) than the starting pair may be either above or below the solvus crest. Incomplete convergence may result either from kinetic limits on the compositional closure or from the intersection with the solvus. These alternatives may be distinguished by a time series study demonstrating either static or evolving compositions and/or by a divergence experiment at the same temperature that shows evolution towards the converging compositions. When converging and diverging pairs reach the same compositional separation, the flanks of the equilibrium solvus are well determined at experimental temperature and pressure.

The first entry in the first section of Table 5, BB945, shows that paired glasses,  $Gr_{10}$  and  $Gr_{60}$ , have become crystalline garnet of a single  $Gr_{35}Py_{65}$  composition at 1300 °C in 2 hours. This is not a convergence because it is unknown *a priori* whether the single garnet composition evolved from a pair of crystalline garnets or from a pair of glasses, which then crystallized from a single glass composition. The former possibility would count as a demonstration of garnet convergence, the second would not. The second entry, BB946, demonstrates that the crystallization process is more rapid than the homogenization process. Paired glasses are recovered as paired crystalline garnets in 6 hours at 1200 °C. The third entry, TT747, demonstrates that 20 hours is sufficient to first crystallize (from the precedent of BB946) and then homogenize (completely converge) the crystalline garnet compositions. Evidently dropping from 1300 to 1200 °C impedes homogenization, as expected for thermally activated diffusion. The TT747 experiment sets the time scale for this process at 1200 °C at ~day rather than hours, unlike at 1300 °C where both

steps were complete in 2 hours, or at 1400 °C, where TT741 (not shown in Table 5) demonstrates completion of both processes in less than 10 minutes. More important, TT747 demonstrates that the consolute  $T_C$  must be below 1200 °C at 6 GPa because complete convergence at the expected consolute composition was achieved, with a day's patience.

The first entry in the 2<sup>nd</sup> section of Table 5, TT750, shows the dramatic slowing of the homogenization rates as temperature drops further to 1100 °C. In 7 days the paired garnet glasses have crystallized without any compositional convergence. We should expect that experimental demonstration of convergence-divergence at 1100 °C will be extremely sluggish. These separate crystalline garnets grown at 1100 °C, 6 GPa form the starting material for a convergence experiment at 1200 °C, 8 GPa, TT766, which produced only modest convergence in 8 days. Treating this product of TT766 to an additional 7 days at 1200 °C, 8 GPa produced the convergent paired garnets of TT767 of  $Gr_{16.5}$  and  $Gr_{38.5}$ . [The garnet compositions are subject to an uncertainty of about  $\pm 2\%$  of Py or Gr component.] Without an additional observation of either longer anneal time or compositional divergence, this result is ambiguous about the location of the solvus.

The third section of Table 5 shows that starting crystalline garnet compositions  $Gr_{22}+Gr_{34}$  diverge to  $Gr_{14}+Gr_{38}$  in 21 days at 1200 °C, 8 GPa in BB991. Given the  $\pm 2\%$  Py or Gr uncertainty on the compositions, this divergence result is indistinguishable from the  $Gr_{16.5}$  and  $Gr_{38.5}$  in the convergence experiment TT767 at the same pressure and temperature condition. Thus we have a very firm location of the flanks of the solvus at 1200 °C, 8 GPa at  $Py_{85}Gr_{15}$  and  $Py_{62}Gr_{38}$ . The XRD patterns appropriate to these convergence and divergence experiments are given in Figure 10. Clearly the solvus in pyrope-grossular is now accessible experimentally.

Sections 4 and 5 of Table 5 show the attempt to demonstrate a similar convergence-divergence at 1100 °C, 8 GPa. The attempt was only partially successful in that convergence and divergence were demonstrated, however the compositional bounds were significantly looser than at 1200 °C, even after experiments of a month's duration (TT875). Clearly the experimental accessibility of the solvus at 1100 °C, 8 GPa is kinetically hindered. It is merely possible to constrain the solvus flanks at 1100 °C to be somewhere between  $\text{Py}_{88}\text{Gr}_{12}$  and  $\text{Py}_{81}\text{Gr}_{19}$  on the pyrope-rich side and  $\text{Py}_{62.2}\text{Gr}_{38.2}$  on the grossular-rich side. It is however possible to draw an important conclusion even from the loose compositional bounds found at 1100 °C. The bounds change very little between 1100 and 1200 °C at 8 GPa! This suggests that 1200 °C is not very close to the consolute  $T_C$ . If 1200 °C were close to  $T_C$ , one would expect the compositional separation of the flanks of the solvus to be more converged at 1200 °C than they are at 1100 °C. That they are not, and because we know (from TT747) that 1200 °C is above  $T_C$  at 6 GPa, we draw the conclusion that  $T_C$  is rising rapidly with P from 6 to 8 GPa. This conclusion is more compatible with our large values for the excess volumes in this series than with the small values found in the literature.

### **Geothermobarometry**

Even small scale but significant deviations from ideal mixing volume may be critical for calculation of high pressure phase equilibrium. Precise data on partial molar volume of garnet components is needed to calculate the equilibrium pressure when using a garnet related geothermobarometry. Therefore, the larger excess volumes we observed here on the join of pyrope-grossular garnet should bring some changes to geothermal barometers with pyrope-grossular garnets.

The partial molar volumes of pyrope and grossular garnet can be calculated by using the

Margules parameters with the following equations (Ganguly et al. 1993):

$$\bar{V}_{pyrope} = \bar{V}_0^{pyrope} + \left[ W_{V_{grossular}} + 2 \left( W_{V_{grossular}} - W_{V_{pyrope}} \right) * X_{pyrope} \right] * X_{grossular}^2 \quad (7a)$$

$$\bar{V}_{grossular} = \bar{V}_0^{grossular} + \left[ W_{V_{pyrope}} + 2 \left( W_{V_{pyrope}} - W_{V_{grossular}} \right) * X_{grossular} \right] * X_{pyrope}^2 \quad (7b)$$

where  $\bar{V}_{pyrope}$  and  $\bar{V}_{grossular}$  are the partial molar volume of end member pyrope and grossular respectively,  $\bar{V}_0^{pyrope}$  and  $\bar{V}_0^{grossular}$  are the standard molar volumes of the end-members at ambient condition,  $X_{pyrope}$  and  $X_{grossular}$  are the mole fractions of the respective components of end members, and  $W_{V_{pyrope}}$  and  $W_{V_{grossular}}$  are the Margules parameters on excess volume.

Partial molar volumes of garnet end-members calculated from equation 7a and 7b are summarized in Figure 11 and compared with those from Ganguly et al. (1993). There is generally satisfactory agreement of our results and those from Ganguly et al. (1993). However in accord with our larger excess volumes,  $V_{pyrope}$  on garnets with Mg-rich composition and  $V_{grossular}$  on garnets with Ca-rich composition, there is disagreement on  $V_{grossular}$  for garnets with Mg-rich composition. Because the partial molar volume of the end member component in the solid solution is larger than the respective molar volume, the equilibrium pressure to be obtained from thermobarometry with pyrope-grossular garnet may be underestimated. Therefore, the volumetric nonideality in the pyrope-grossular join needs to be considered in applications of geotherm barometry.

## Back reflections

The excess volumes in the pyrope-grossular garnet series are positive. Dry garnet excess volumes are larger than when they are damp. Neither dry nor damp garnet pyrope-grossular solutions are particularly well described by the Margules model. Yet the binary Margules model

seems to predict the rise of the solvus with pressure. Our dry garnets produce experimentally observable reversible exsolution at pressure and temperature condition consistent with the large excess volumes we measure on our dry garnets. Like the chlorides, the Margules description fails to describe well the excess volume data itself, but provides, paradoxically, an adequate tool for predicting the evolution of the solvus with pressure, a much more sensitive metric of solution properties.

### **ACKNOWLEDGMENTS**

This work was supported by the U.S. National Science Foundation. The Advanced Light Source is supported by the Director, Office of Science, Office of Basic Energy Sciences, of the U.S. Department of Energy under Contract No. DE-AC02-05CH11231 at Lawrence Berkeley National Laboratory. We thank George Harlow from the Museum of Natural History for help with XRD measurements. We thank Jean Hanley and Jinyuan Yan for their technical assistance.

### **REFERENCES CITED**

- Bosenick, A., and Geiger, C.A. (1997) Powder X-ray diffraction study of synthetic pyrope-grossular garnets between 20 and 295 K. *Journal of Geophysical Research*, 102, 22649-22657.
- Bosenick, A., Geiger, C.A., and Cemic, L. (1996) Heat capacity measurements of synthetic pyrope-grossular garnets between 320 and 1000 K by differential scanning calorimetry. *Geochimica et Cosmochimica Acta*, 60, 3215-3227.

- Bosenick, A., Geiger, C.A., and Phillips, B.L. (1999) Local Ca-Mg distribution of Mg-rich pyrope-grossular garnets synthesized at different temperatures revealed by  $^{29}\text{Si}$  MAS NMR spectroscopy. *American Mineralogist*, 84, 1422-1432.
- Bosenick, A., Dove, M.T., and Geiger, C.A. (2000) Simulation studies in the pyrope-grossular solid solution series. *Physics and Chemistry of Minerals*, 27, 398-418.
- Bosenick, A., Geiger, C.A., Schaller, T., and Sebald, A. (1995) A  $^{29}\text{Si}$  MAS NMR and IR spectroscopic investigation of synthetic pyrope-grossular garnet solid solutions. *American Mineralogist*, 80, 691-704.
- Bosenick, A., Dove, M.T., Heine, V., and Geiger, C.A. (2001) Scaling of thermodynamic mixing properties in garnet solid solutions. *Physics and Chemistry of Minerals*, 28, 177-187.
- Cheary, R.W., and Coelho, A.A. (1996) Programs XFIT and FOURYA, deposited in CCP14 powder diffraction library. Engineering and Physical Sciences Research Council, Daresbury Laboratory, Warrington, England.
- Clark, S.M. (1996) A new energy dispersive powder diffraction facility at the SRS. *Nuclear Instruments and Methods in Physics Research*, A381, 161-168.
- Cockcroft, J.K., and Barnes, P. (1997) Powder diffraction on the web, originally an internet-based advanced certificate course offered by Birkbeck College, but with the static course material since released on the group's web site: <http://pd.chem.ucl.ac.uk/pd/welcome.htm>.
- Cressy, P. (1978) Exsolution in almandine-pyrope-grossular garnet. *Nature*, 271, 533-534.
- Dachs, E., and Geiger, C.A. (2006) Heat capacities and entropies of mixing of pyrope-grossular ( $\text{Mg}_3\text{Al}_2\text{Si}_3\text{O}_{12}$ - $\text{Ca}_3\text{Al}_2\text{Si}_3\text{O}_{12}$ ) garnet solid solutions: A low-temperature calorimetric and a thermodynamic investigation. *American Mineralogist*, 91, 894-906.

- Dapiaggi, M., Geiger, C.A., and Artioli, G. (2005) Microscopic strain in synthetic pyrope-grossular solid solutions determined by synchrotron X-ray powder diffraction at 5 K: The relationship to enthalpy of mixing behavior. *American Mineralogist*, 90, 506-509.
- Du, W., Clark, S.M., and Walker, D. (2015) Thermo-compression of pyrope-grossular garnet solid solution: non-linear compositional dependence. *American Mineralogist*, 100, 215-222.
- Freeman, C.L., Allan, N.L., and van Westrenen, W. (2006) Local cation environments in the pyrope-grossular  $Mg_3Al_2Si_3O_{12}$ - $Ca_3Al_2Si_3O_{12}$  garnet solid solution. *Physical Review B*, 74, 134203.
- Ganguly, J., and Kennedy, G.C. (1974) The energetics of natural garnet solid solution I. Mixing of the aluminosilicate end-members. *Contributions to Mineralogy and Petrology*, 48, 137-148.
- Ganguly, J., Cheng, W., and O'Neill, H.C. (1993) Syntheses, volume, and structural changes of garnets in the pyrope-grossular join; implications for stability and mixing properties. *American Mineralogist*, 78, 583-593.
- Ganguly, J., Cheng, W., and Tirone, M. (1996) Thermodynamics of aluminosilicate garnet solid solution: new experimental data, an optimized model, and thermometric applications. *Contributions to Mineralogy and Petrology*, 126, 137-151.
- Geiger, C.A., and Feenstra, A. (1997) Molar volumes of mixing of almandine-pyrope and almandine-spessartine garnets and the crystal chemistry and thermodynamic-mixing properties of the aluminosilicate garnets. *American Mineralogist*, 82, 571-581.

- Geiger, C.A., Newton, R.C., and Kleppa, O.J. (1987) Enthalpy of mixing of synthetic almandine-grossular and almandine-pyrope garnets from high-temperature solution calorimetry. *Geochimica et Cosmochimica Acta*, 51, 1755-1763.
- Hammersley, A.P., Svensson, S.O., Hanfland, M., Fitch A.N., and Häusermann, D. (1996) Two-dimensional detector software: from real detector to idealised image or two-theta scan. *High Pressure Research*, 14, 235-248.
- Haselton, H. T. and Newton, R. C. (1980) Thermodynamics of pyrope-grossular garnets and their stabilities at high temperatures and high pressures. *Journal of Geophysical Research*, 85, 6973-6982.
- Hazen, R.M., and Navrotsky, A. (1996) Effects of pressure on order-disorder reactions. *American Mineralogist*, 81, 1021–1035.
- Johnson, M.C., Walker, D., Clark, S.M., and Jones, R.L. (2001) Thermal decomposition of rhombohedral  $\text{KClO}_3$  from 29–76 kilobars and implications for the molar volume of fluid oxygen at high pressures. *American Mineralogist*, 86, 1367–1379.
- Iiyama, J.T. (1974) Substitution, déformation locale de la maille et équilibre de distribution des éléments en traces entre silicates et solution hydrothermate. *Bull Bulletin de la Société française de minéralogie et de cristallographie*, 97, 143-151.
- Kelsey, K.E., Stebbins, J.F., Du, L., Mosenfelder, J.L., Asimow, P.D., and Geiger, C.A. (2008) Cation order/disorder behavior and crystal chemistry of pyrope-grossular garnets: An  $^{17}\text{O}$  3QMAS and  $^{27}\text{Al}$  MAS NMR spectroscopic study. *American Mineralogist*, 93, 134-143.
- Langford, J.I. (1978) A rapid method for analyzing the breadths of diffraction and spectral lines using the Voigt function. *Journal of Applied Crystallography*, 11, 10-14.

- Langford, J.I., and Wilson, A.J.C. (1978) Scherrer after sixty years: a survey and some new results in the determination of crystallite size. *Journal of Applied Crystallography*, 11, 102-113.
- Newton, R.C., and Wood, B.J. (1980) Volume behavior of silicate solid solution. *American Mineralogist*, 65, 733-745.
- Newton, R.C., Charlu, T.V., and Kleppa, O.J. (1977) Thermochemistry of high pressure garnets and clinopyroxenes in the system CaO-MgO-Al<sub>2</sub>O<sub>3</sub>-SiO<sub>2</sub>. *Geochimica et Cosmochimica Acta*, 41, 369-377.
- Shannon, R.D. (1976) Revised effective ionic radii and systematic studies of interatomic distances in halides and chalcogenides. *Acta Crystallographica*, A32, 751-767.
- Scherrer, P. (1918) Bestimmung der Grösse und der inneren Struktur von Kolloidteilchen mittels Röntgenstrahlen. *Nachrichten der Kgl Gesellschaft der Wissenschaftern zu Göttingen*, 26, 98-100.
- Stokes, A.R., and Wilson, A.C. (1944) The diffraction of X rays by distorted crystal aggregates. *Proceedings of the Physical Society*, 56, 174-181.
- Thompson, J.B. (1967) Thermodynamic properties of simple solutions. In P.H. Abelson, *Advances in Geochemistry*, 2, 340-361.
- Ungaretti, L., Leona, M., Merli, M., and Oberti, R. (1995) Non-ideal solid-solution in garnet; crystal-structure evidence and modeling. *European Journal of Mineralogy*, 7, 1299-1312.
- Vinograd, V.L., Sluiter, M.H.F, Winkler, B., Putnis, A., Hålenius, J.D.G., and Becker, U. (2004) Thermodynamics of mixing and ordering in pyrope-grossular solid solution. *Mineralogical Magazine*, 68(1), 101-121.

- Walker, D., Clark, S.M., Jones, R.L., and Cranswick, L.M. (2000) Rapid methods for the calibration of solid-state detectors. *Journal of Synchrotron Radiation*, 7, 18–21.
- Walker, D., Cranswick, L.M.D., Verma, P.K., Clark, S.M., and Buhre, S. (2002) Thermal equations of state for B1 and B1 KCl. *American Mineralogist*, 87, 805–812.
- Walker, D., Verma, P.K., Cranswick, L.M.D., Clark, S.M., Jones, R. L., and Buhre, S. (2005) Halite-sylvite thermoconsolution. *American Mineralogist*, 90, 229-239.
- Wang, L., Essene, E.J., and Zhang, Y. (2000) Direct observation of immiscibility in pyrope-almandine-grossular garnet. *American Mineralogist*, 85, 41-46.
- Williamson, G.K., and Hall, W.H. (1953) X-ray broadening from filled aluminium and wolfram. *Acta Metallurgica* 1, 22-31.
- Wood, B.J. (1988) Activity measurements and excess entropy-volume relationships for pyrope-grossular garnets. *Journal of Geology*, 96, 721-729.

**TABLE 1.** Unit cell parameter of quenched end members pyrope and grossular garnets from different studies that show agreement among the studies, including our MA synthesis garnets.

Experiment	Temperature (°C)	Pressure (GPa)	Composition	Unit cell parameter (Å)	Reference
Multi Anvil	1400	6	Grossular	11.850(1)	This study
			Pyrope	11.454(1)	
Piston Cylinder	1300	4	Grossular	11.849(1)	Newton et al. (1977)
			Pyrope	11.457(1)	
	1350-1400	4 - 4.2	Grossular	11.852(1)	Ganguly et al. (1993)
			Pyrope	11.457(1)	
1400	3	Grossular	11.851(1)	Bosenick and Geiger (1997)	
		Pyrope	11.455(1)		

**TABLE 2.** The excess volume and microstrain of pyrope-grossular garnet solutions synthesized from dry glass in MA (6GPa, 1400 °C)\*

Composition	a (Å)	V(Å <sup>3</sup> )	Molar volume (cm <sup>3</sup> /mole)	Excess V (cm <sup>3</sup> /mole)	Microstrain* (10 <sup>-4</sup> )
Pyrope	11.454(1)	1502.7(8)	113.08(6)	0	1.7(3)
Py <sub>80</sub> Gr <sub>20</sub>	11.542(1)	1539.2(4)	115.82(3)	0.20(3)	10.1(3)
Py <sub>60</sub> Gr <sub>40</sub>	11.644(1)	1578.7(4)	118.80(3)	0.87(3)	6.4(5)
Py <sub>40</sub> Gr <sub>60</sub>	11.726(1)	1612.3(4)	121.33(3)	0.97(3)	1.5(4)
Py <sub>20</sub> Gr <sub>80</sub>	11.787(1)	1637.6(4)	123.23(3)	0.44(3)	9.9(4)
Grossular	11.850(4)	1664.0(8)	125.22(6)	0	0(6)

\*All of the unit cell parameter data present in this table were measured by XRD in DAC at ALS, Lawrence Berkeley National Lab. The values in parentheses represent the uncertainties in the last digits.

**TABLE 3.** P-T-t conditions of different syntheses experiments on Py<sub>60</sub>Gr<sub>40</sub>\*

Experiment	Starting material	Pressure (GPa)	Temperature (°C)	Heating time (Minutes)	Molar Volume (cm <sup>3</sup> /mole)	Microstrain (10 <sup>-4</sup> )
TT717	glass	6	1400	205	118.76(2)	8.5(4)
TT734	seeded glass	4	1300	180	118.43(1)	5.4(4)
TT736	seeded glass	4	1300	150	118.59(1)	4.2(3)
BB941	seeded glass	6	1400	60	118.40(2)	6.2(4)

\* Experiments TT734, TT736 and BB941 started from the same seeded glass powder, and the garnet seed was prepared with hydrothermal assistance as described by Bosenick et al. (1995). TT736 encased in Pt capsule. All the quenched garnet crystals were checked by XRD on RIGAKU at American Museum of Natural History. The values in parentheses represent the uncertainties in the last digits.

**TABLE 4.** Unit cell parameters of garnet crystals with composition Py<sub>80</sub>Gr<sub>20</sub>\*

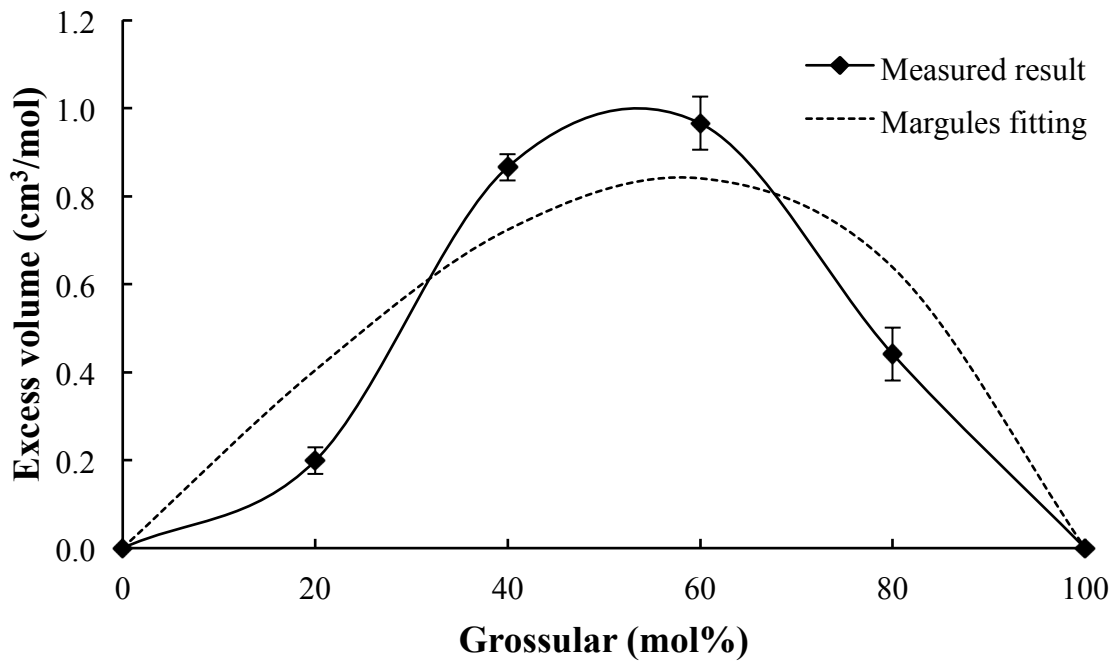
Experiment	Starting material	Temperature (°C)	Heating time (Minutes)	Unit cell parameter (Å)	Microstrain (10 <sup>-4</sup> )
TT 724	glass	1400	30	11.542(1)	10.1(3)
TT890	glass	1300	5	11.543(1)	3.6(3)
TT895B	TT890	1400	100	11.540(1)	10.2(3)

All of the garnets in this table are quenched samples synthesized in MA device at LDEO at 6 GPa. Microstrain data were calculated from XRD profiles collected at ALS, Lawrence Berkeley National Lab. The values in parentheses represent the uncertainties in the last digits.

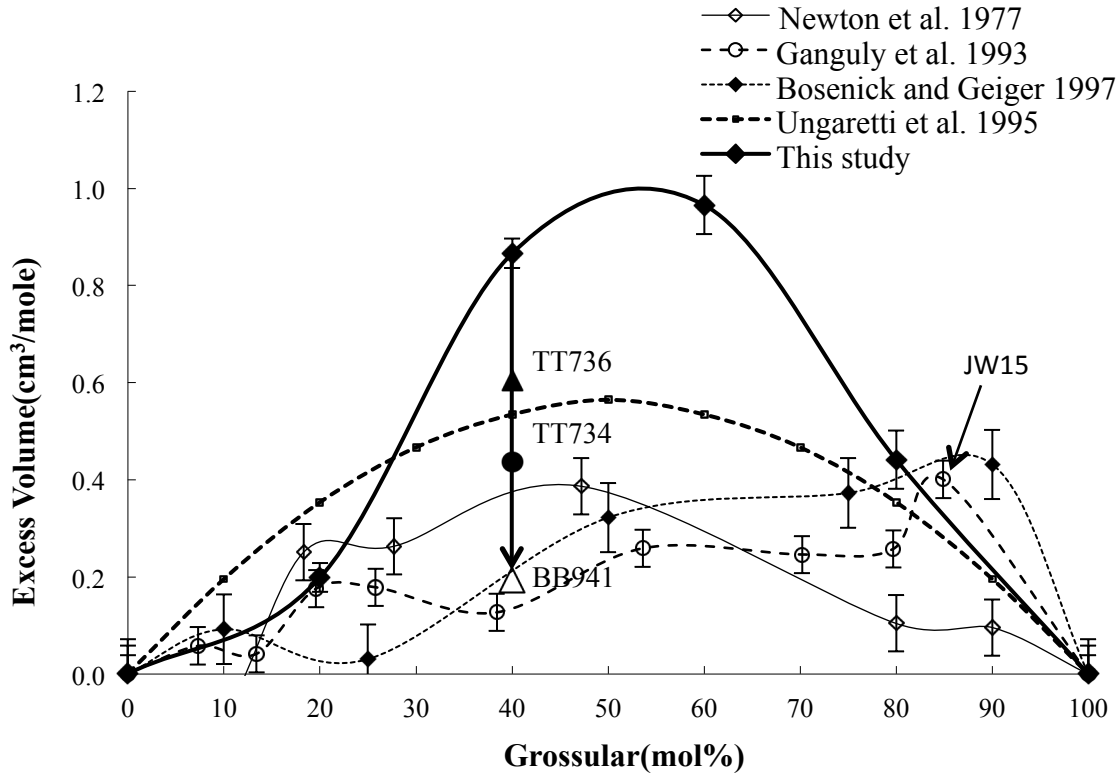
**TABLE 5.** P-T-t conditions of two-phase garnet annealing experiments\*

Experiment	Starting material	Pressure (GPa)	Temperature (°C)	Heating time	Composition of products
Preliminary experiments, 6 GPa					
BB945	Glass mixture (Gr <sub>10</sub> +Gr <sub>60</sub> 1:1 wt%)	6	1300	2 hours	~Gr <sub>35</sub>
BB946	as above	6	1200	6 hours	Gr <sub>10</sub> +Gr <sub>60</sub>
TT747	as above	6	1200	20 hours	~Gr <sub>35</sub>
Convergence experiment, 1200 °C, 8 GPa					
TT750	Glass mixture (Gr <sub>10</sub> +Gr <sub>60</sub> 1:1 wt%)	6	1100	7 days	Gr <sub>10</sub> +Gr <sub>60</sub>
TT766	Product of TT750	8	1200	8 days	Gr <sub>12</sub> +Gr <sub>43</sub> +Gr <sub>53</sub>
TT767	Product of TT766	8	1200	7 days	Gr <sub>16.5</sub> +Gr <sub>38.5</sub>
Divergence experiment, 1200 °C, 8 GPa					
BB980	Glass mixture (Gr <sub>20</sub> +Gr <sub>40</sub> 1:1 wt%)	6	1150	0.5 hours	Gr <sub>22</sub> +Gr <sub>34</sub>
BB991	Product of BB980	8	1200	21 days	Gr <sub>14</sub> +Gr <sub>38</sub>
Convergence experiment, 1100 °C, 8 GPa					
BB970	Glass mixture (Gr <sub>10</sub> +Gr <sub>60</sub> 1:1 wt%)	6	1200	1 hour	Gr <sub>10</sub> +Gr <sub>60</sub>
BB974	Product of BB970	8	1100	24 days	Gr <sub>12.5</sub> + Gr <sub>39</sub>
Semidivergence experiment, 1100 °C, 8 GPa					
BB977	Glass mixture (Gr <sub>20</sub> +Gr <sub>40</sub> 1:1 wt%)	6	1150	0.5 hours	Gr <sub>20</sub> +Gr <sub>40</sub>
TT875	Product of BB977	8	1100	33 days	Gr <sub>19</sub> +Gr <sub>36</sub>

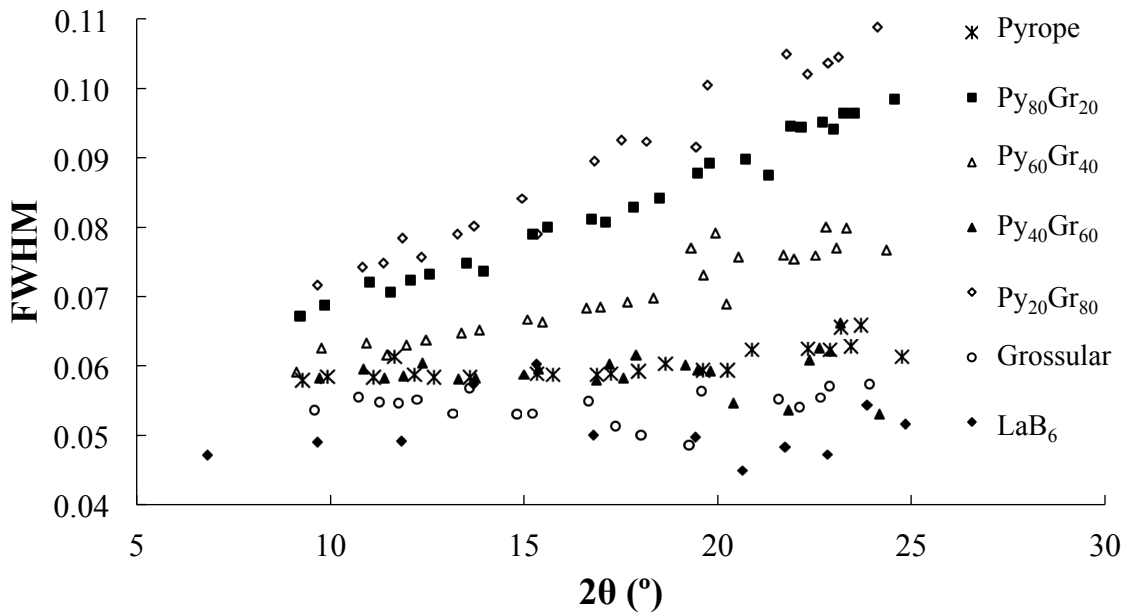
\* Composition of the coexisting garnet phases were estimated by comparing the XRD peak position with the pyrope-grossular binary. XRD was done at the American Museum of Natural History by using CuK $\alpha$  radiation ( $\lambda=1.540562$ ) on RIGAKU (46 kV and 40 mA). Uncertainties on the garnet compositions are  $\pm 2$  Gr or Py % units.



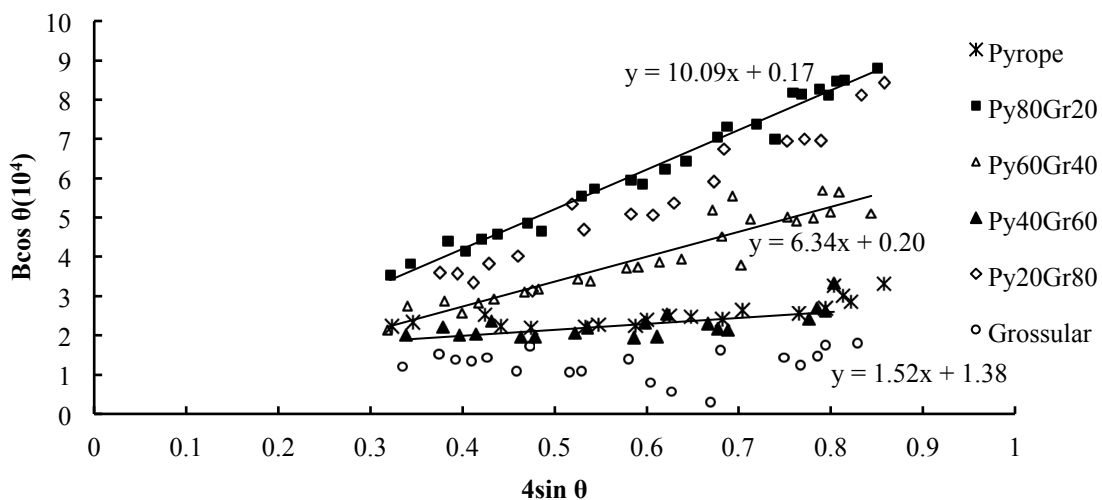
**FIGURE 1.** Margules equation fitted to excess volume of garnet on pyrope-grossular join. The binary Margules equation was used to approximately fit the asymmetric excess volume calculated from garnet synthesized in multi-anvil (MA). The error bars were calculated from uncertainties from the molar volume data in Table 2.



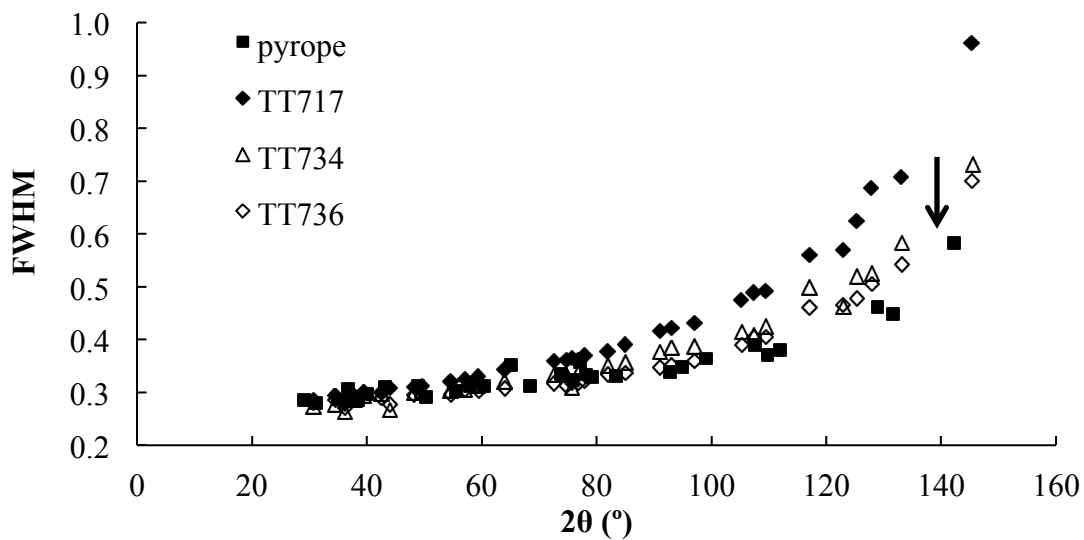
**FIGURE 2.** Excess volumes of the pyrope-grossular garnet solid solution. Positive excess volumes were determined across the whole pyrope-grossular join. The modeling by Ungaretti et al. (1995) shows a symmetrical positive excess volume along this binary. Our study (garnets synthesized dry in multi-anvil (MA) techniques at LDEO) shows the largest excess volume, about 3 times of that from garnets synthesized in piston cylinder reported by Newton et al. (1977), Ganguly et al. (1993), and Bosenick and Geiger (1997), and a more symmetrical shape. The error bars refer to the standard error from least squares fitting procedure for the unit cell volume. The values for experiments TT734, TT736, and BB941 show typical drops in the excess volume experienced with dampness caused by use of hydrothermally grown seeds. It is possible that the JW15 experiment of Ganguly et al. (1993) may have leaked or lost its moisture, because it plots on our dry curve. The error bars for the literature studies represent one standard deviation.



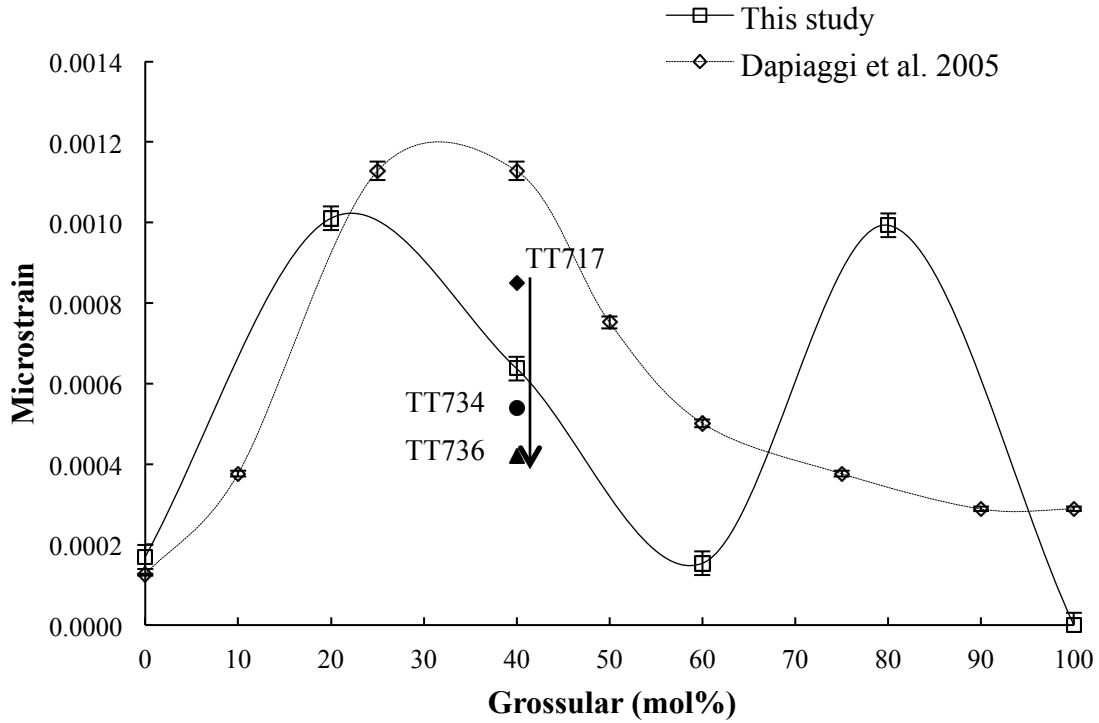
**FIGURE 3.** The FWHM values from Pseudo-Voigt fitting: garnet solid solutions with intermediate compositions show much broader X-ray peaks than the two end members pyrope and grossular. XRD peak broadening changes linearly with Bragg angle over this limited range of  $2\theta$ .



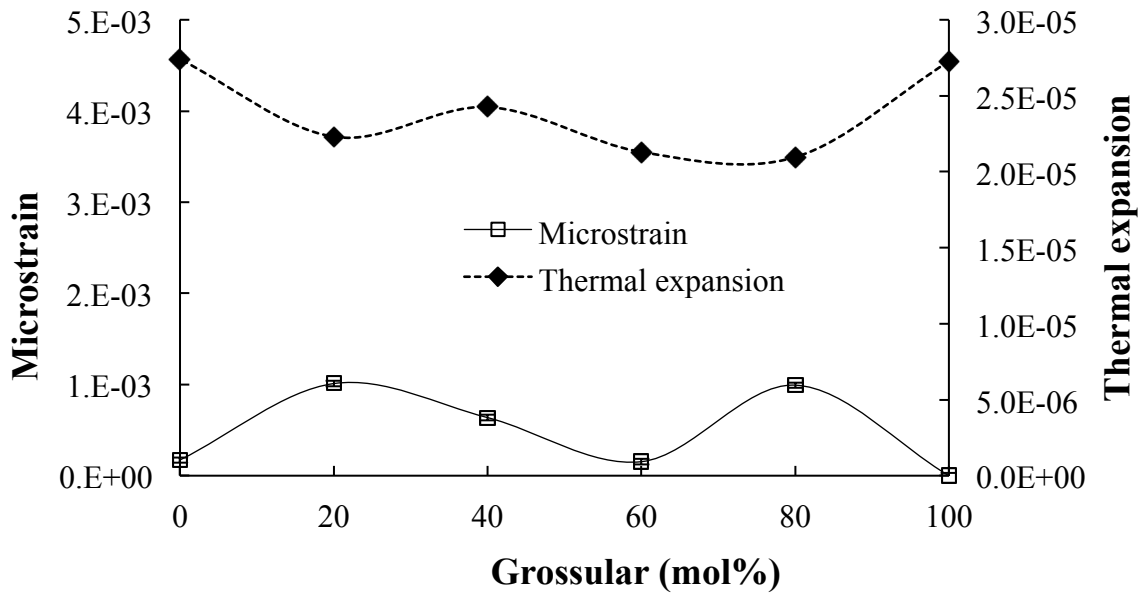
**FIGURE 4.** Williamson-Hall plot for XRD peak widening data of pyrope-grossular garnet solid solutions. The slope of the fitting equation (equation 5) represents the contribution of microstrain to the XRD peak broadening.



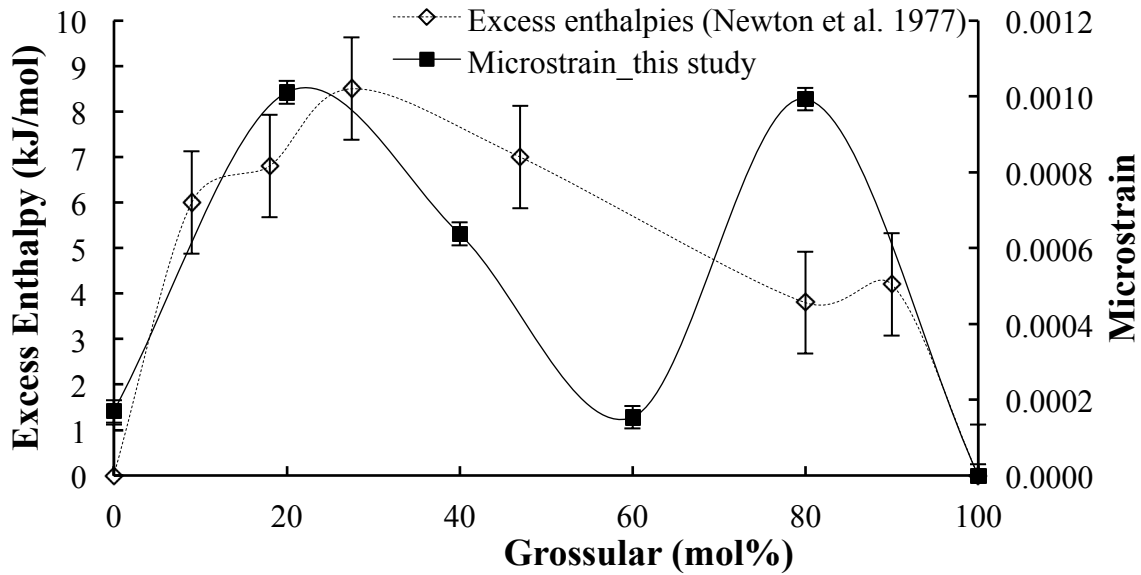
**FIGURE 5.** The FWHM values from Pseudo-Voigt fitting: garnet solid solutions with composition  $\text{Py}_{60}\text{Gr}_{40}$  synthesized with hydrothermal assistance (TT734 and TT736) show narrower X-ray peaks (smaller FWHM values as the arrow showing) than those synthesized from dry glass (TT717). Pyrope with less peak broadening (see Figure 3) is shown for comparison. FWHM values, array curvatures, and the range of  $2\theta$  shown here are larger than in Figure 3 because the AMNH RIGAKU instrument has a different response and collection aperture from the ALS 12.2.2 end station.



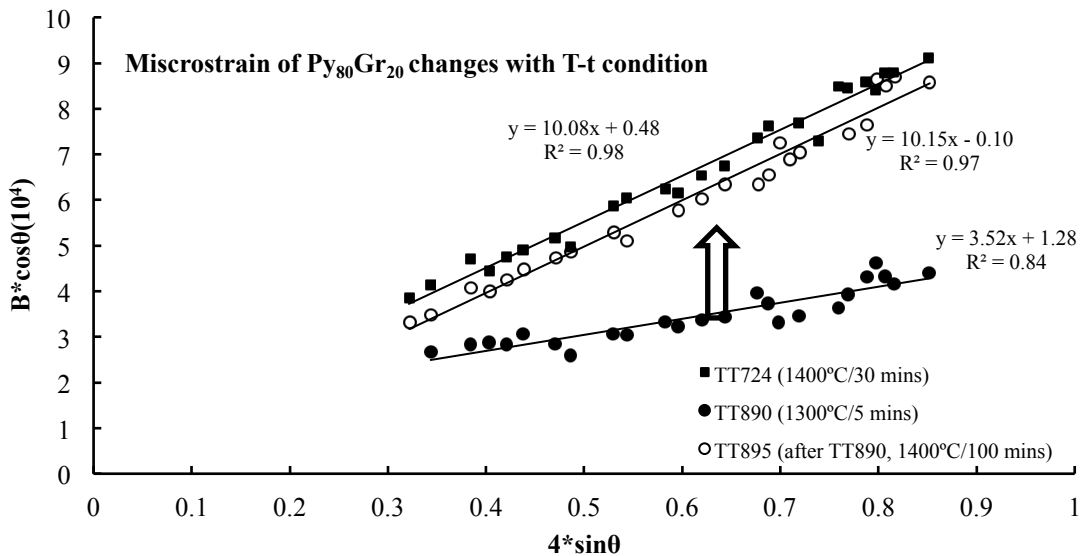
**FIGURE 6.** Microstrain inside garnet structure calculated from X-ray peak broadening along the pyrope-grossular join (Table 2). Similar measurable peak broadening was reported by Dapiaggi et al. (2005), except for garnets with intermediate composition close to the grossular end. The microstrain of TT717, TT734, and TT736 was calculated from FWHM values showed in Figure 5, showing the possible effect of dampness on microstrain, releasing microstrain as the arrow shows. The calculated microstrain value for TT717 (0.00085) is different from the base line (0.00064) because these XRD data were collected at AMNH, and the RIGAKU instrument has a different response and collection aperture from the ALS 12.2.2 end station.



**FIGURE 7.** A good anti-correlation is observed between thermal expansion (from our companion paper, Du et al. 2015) and microstrain value calculated from XRD peak width. For example, garnets with composition  $\text{Py}_{80}\text{Gr}_{20}$  (Mg:Ca=4:1) and  $\text{Py}_{20}\text{Gr}_{80}$  (Mg:Ca=1:4) show smaller thermal expansion and the widest XRD peaks, and garnets with most intermediate composition  $\text{Py}_{40}\text{Gr}_{60}$  show large thermal expansion but small microstrain value.

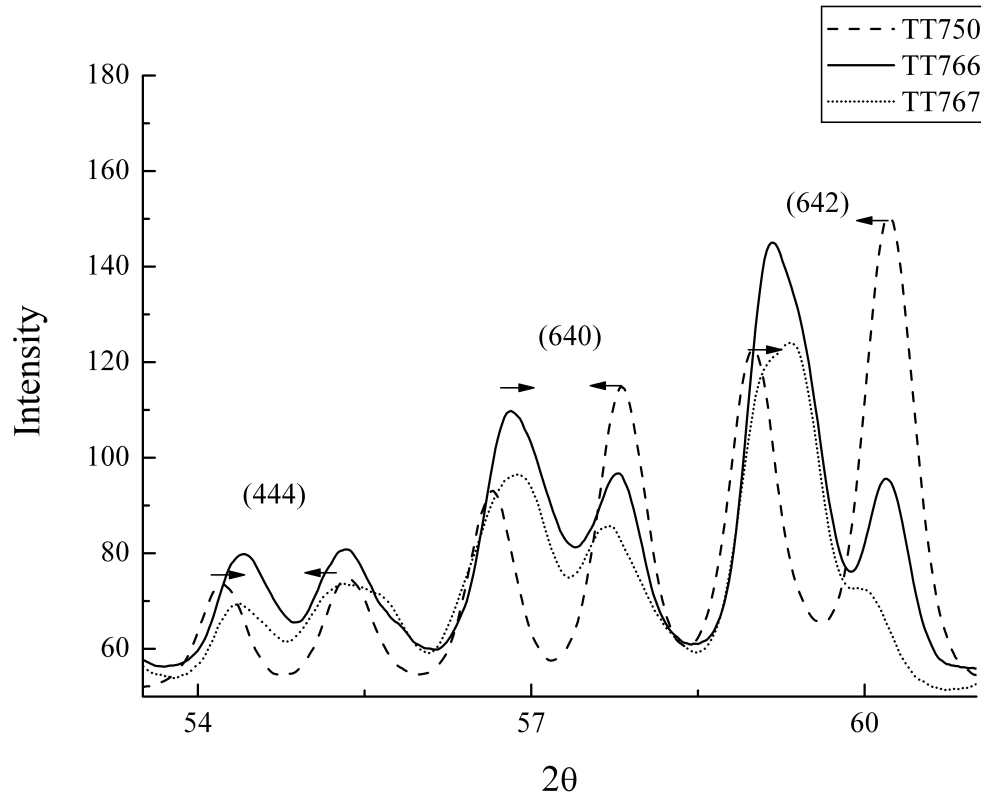


**FIGURE 8.** A correlation is observed between microstrain and the excess mixing enthalpy reported by Newton et al. (1977). The error bars for excess enthalpies represent one standard deviation. The error bars for microstrain data were present in Table 2.



**FIGURE 9.** Experimental results show how the second round annealing at higher temperature affect the XRD peak width. All three experiments were done in MA apparatus at 6 GPa. TT890 is garnet synthesized from glass and heated at 1300 °C for 5 minutes; TT895 is reheating product of experiment TT890 at 1400 °C for 100 minutes (Table 4). Higher strains go with higher temperatures and relatively smaller unit cell volume. This combination of properties can be

shown to develop for garnets originally grown quickly at 1300 °C and then annealed at 1400 °C where microstrain grows (TT-895).



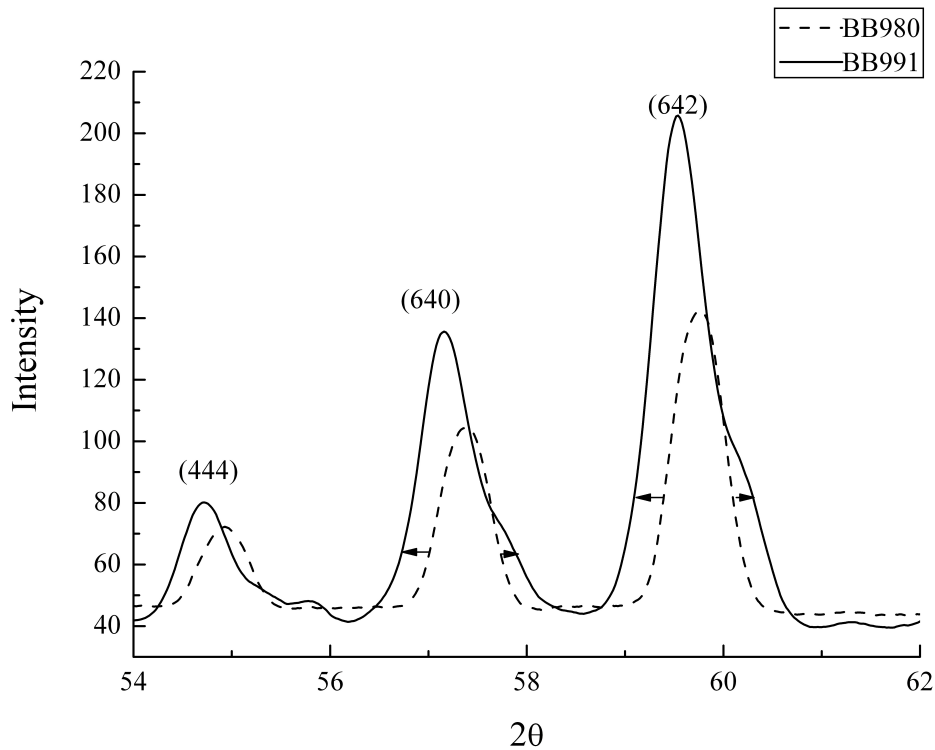


**FIGURE 10.** XRD patterns of two coexisting garnet phases collected at the American Museum of Natural History by using  $\text{CuK}\alpha$  radiation ( $\lambda=1.540562$ ) on RIGAKU (46 mV and 40 mA). Position of the peaks (444), (640), and (642) moved during long time annealing at 8 GPa and 1200°C. The movements toward different directions (both convergence and divergence) of the XRD peaks indicate reversible exsolution of garnet at these PT conditions. The flanks of the solvus at 1200 °C, 8 GPa are located at  $\text{Py}_{85.2}\text{Gr}_{15.2}$  and  $\text{Py}_{62.2}\text{Gr}_{38.2}$ .

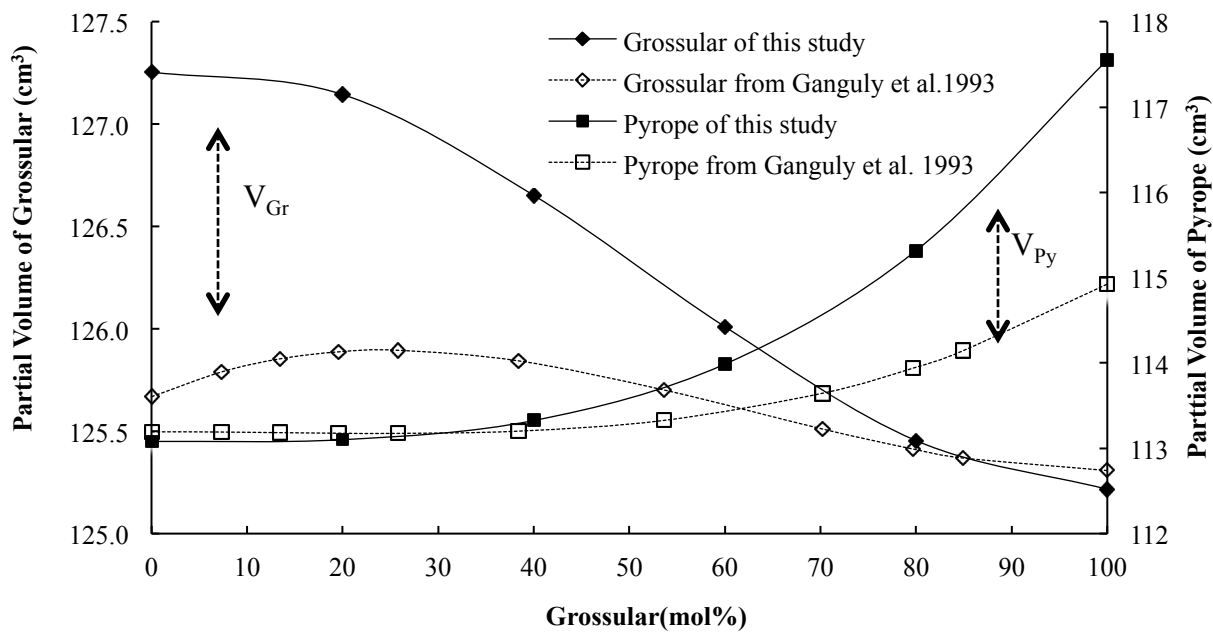


**FIGURE 11.** Partial molar volumes of end-member components in the pyrope-grossular solid solutions. Our result (solid line) calculated from the larger excess volume that we present in this paper is different from that of Ganguly et al. (1993) (dash line) in the case of  $V_{Gr}$  in pyrope rich end and  $V_{Py}$  at grossular rich end.